Acoustic emission spikes at workpiece edges in grinding: Origin and applications

R. Babel, P. Koshy *
Department of Mechanical Engineering, McMaster University, Hamilton, Canada

M. Weiss
Laboratory for Machine Tools and Production Engineering
RWTH Aachen University, Aachen, Germany

Abstract

Acoustic emission signals from interrupted machining operations exhibit spikes at workpiece entry and exit, which are particularly conspicuous in grinding. Although their occurrence has been widely reported, these spikes are yet to be clarified in terms of their origin or interpreted to yield useful process information. This paper hence reports on the analyses of time-averaged and raw acoustic emission signals from surface grinding, with reference to burr formation as well as dynamic and thermal effects, in order to elucidate this intriguing phenomenon. The transient spikes at the entry and exit are shown to be a consequence of the wheel establishing and losing contact with the work over the actual contact length, in terms of heat conduction and damping, which are reflected in characteristic frequency bands of the AE signal. The research is demonstrated to have consequently yielded a simple, non-destructive method for assessing the actual wheel-work contact length in grinding.

Key words: acoustic emission, burr formation, contact length, grinding burn, process monitoring

1 Introduction

In light of its superior sensitivity to the multitude of fine dynamic interactions between the wheel and the workpiece, acoustic emission (AE) has emerged as a valuable tool in a host of monitoring applications in grinding. Typical examples include in-process wheel mapping [1], and the sensing of wheel-work contact, wheel loading, chatter and thermal damage [2,3].

* Corresponding author
Email address: koshy@mcmaster.ca (P. Koshy).

Grinding-induced AE comprises features pertaining to such phenomena as chip formation, friction, grit/bond fracture and thermo-mechanically activated phase transitions, and accordingly entails both continuous and burst type features. In many applications, it suffices to examine the signal in terms of time-averaged indices, while others necessitate frequency domain analyses of the raw AE signal, as the relevant information is embedded in the spectral components of the signal. In either case, due to the complex nature of grinding processes, the challenge in the effective and reliable application of AE lies in the identification and interpretation of signatures pertinent to the process responses that are of interest.

An intriguing aspect of AE generated in interrupted machining operations is the manifestation of spikes at the workpiece entry and exit edges, which are particularly conspicuous in grinding. Fig. 1 depicts typical root mean square (RMS) representations of the AE signal, and the corresponding acceleration and force signals acquired in a direction normal to the generated surface, in a single pass of a surface grinding operation. Relative to the acceleration and force signals, the spikes at either ends of the AE signal can be seen to be markedly obvious and distinct. As will be shown later, depending on the workpiece edge geometry, the amplitude of the spikes that flank the continuous segment of the AE signal can in perspective be many times larger.

The spikes have been reported in several publications related to cutting [4,5] and grinding [6,7], as well as wheel dressing [3]. In cutting, the spikes have been attributed [4] to the impact and material ploughing associated with cut entry, and to the rapid unloading and chip breaking at the cut exit, noting further that the trends are consistent with the variation in the principal stresses on the tool rake face. As for grinding, hypotheses such as the reflection of standing AE waves [3], incipient chip formation at the entry and elastic deformation of the wheel-work interface at the exit [6], and an increased gain at the edges associated with the acoustic response of the system [7] have been postulated towards explaining their incidence.

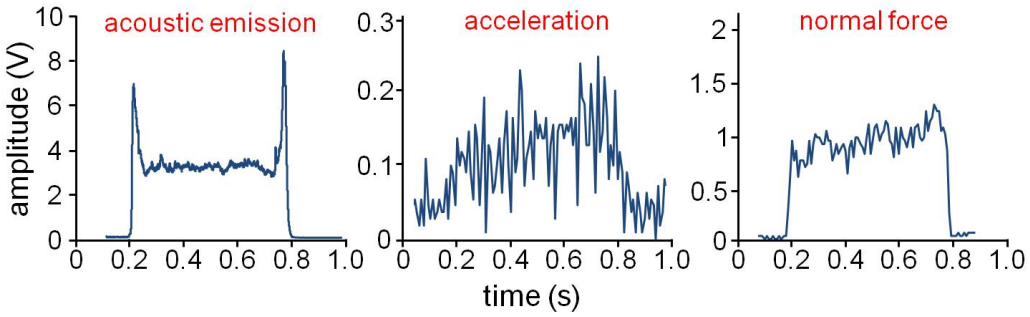

Fig. 1. Qualitative comparison of the root mean square acoustic emission, acceleration and normal force signals.

In view of the tentative nature of the premises above and the lack of a detailed specific investigation to this end, the focus of the research reported in this paper was on inquiring into the origin of the AE spikes, with reference to entry and exit in a surface grinding process. The research emphasis was on comprehending the occurrence of spikes in fundamental terms, with a view to gaining possibly unique and useful process information that they may encapsulate. What embarked as a curiosity-driven research is shown in this paper to have resulted in a simple, effective and novel method for assessing the actual wheel-work contact length, which is a parameter that is of much fundamental significance in grinding.

2 Experimental

Considering that the occurrence of the AE spikes corresponded to the workpiece entry and exit, the underlying mechanisms were hypothesized to have their origins in the following phenomena that pertain to workpiece edges: (i) burr formation, (ii) thermally-induced alterations to the workpiece material, and (iii) dynamic effects associated with the engagement and disengagement of the wheel with the workpiece.

To the end of testing these hypotheses, experiments involved wet plunge surface grinding of hardened (55 HRC) high speed steel workpieces using a vitrified-bonded aluminum oxide wheel. A geometrical parameter that significantly influences the three aforementioned phenomena is the wedge angle of the workpiece at entry and exit. This angle was hence varied over a range of 45° to 175° to investigate its influence on the structure of the AE spikes, with a view to gaining an insight into the spike occurrence. The spikes were further examined with reference to the grinding direction and the wheel depth of cut. The baseline operating conditions involved up-grinding at a wheel speed v_s of 20 m/s, a table feed v_w of 10.2 m/min, a depth of cut a_e of 10 μm, and a width of cut b_w of 10 mm, unless noted otherwise.

The AE signal was acquired using a broadband Kistler 8152B sensor with a fairly flat response in the frequency range of 50 kHz to 400 kHz. The sensor was magnetically clamped to the vice holding the workpiece, midway along its length in consideration of the moving AE source. AE emanating from the process was analyzed in both the time averaged RMS form and in terms of its frequency content. The RMS AE signal entailed an integration time constant of 1.2 ms and was digitized at a sampling rate of 20 kHz. The raw AE signal was band-pass filtered between 50 kHz and 1000 kHz, and recorded at a rate of 2 MHz. The results of experiments that were designed and executed expressly to test the proposed hypotheses and resolve the effects are detailed in the following.

3 Results and discussion

It is to be noted that due consideration of certain aspects of AE signal acquisition and processing is essential in order to realize the spikes in the RMS domain. Firstly, the time constant used in the calculation of the RMS signal need be small relative to the duration of the spike, but for which the spikes will fail to materialize due to the averaging effect of RMS calculations. The time constant of 1.2 ms used in the present work is well over an order of magnitude lower than the typical durations over which the spikes were observed to be sustained, for the grinding conditions employed in this research. Secondly, for a given sensor location, the amplifier gain need be low enough to ensure that the raw AE signal is not saturated at any time, so as to preclude any signal distortion from masking the spikes.

3.1 Analysis of RMS AE signal

During the initial phase of this work, measurements conducted using a tactile instrument to characterize the form and surface roughness indicated no significant local deviations in the vicinity of the workpiece entry and exit edges, corresponding to the spike locations. Subsequent work focused on burr formation that tends to manifest particularly at workpiece edges, with a view to investigating a possible link.

Preliminary up-grinding tests indicated evidence to this end in that both burr formation and the magnitude of the spikes at the exit edge were found to gradually attenuate with each grinding pass, following the first pass during which both burr formation and the spike height were comparatively significant. Deburring of the workpiece in between passes was further observed to stimulate burr formation in the subsequent grinding pass and concomitantly manifest a corresponding increment in the spike height.

Considering the disparity known to exist in the formation of burrs at the entry and exit edges, the effect of grinding direction was hence investigated, the results of which are shown in Fig. 2. Entry and exit as stated here relate to the workpiece, and refer to its engagement and disengagement with the wheel, respectively. The feature of particular note in Fig. 2 is the magnitude of the spike, in general, being relatively higher at the exit edge in up-grinding and at the entry edge in down-grinding. This may be deemed to be a consequence of exit and entry burrs being significant in up-grinding and down-grinding, respectively, as reported in [8]. As shown schematically in the figure, the process kinematic in up-grinding tends to deform the material into the workpiece at the entry edge inhibiting burr formation therein, while promoting its flow away from the workpiece at the exit edge, resulting in significant exit burrs. The converse holds true for down-grinding.

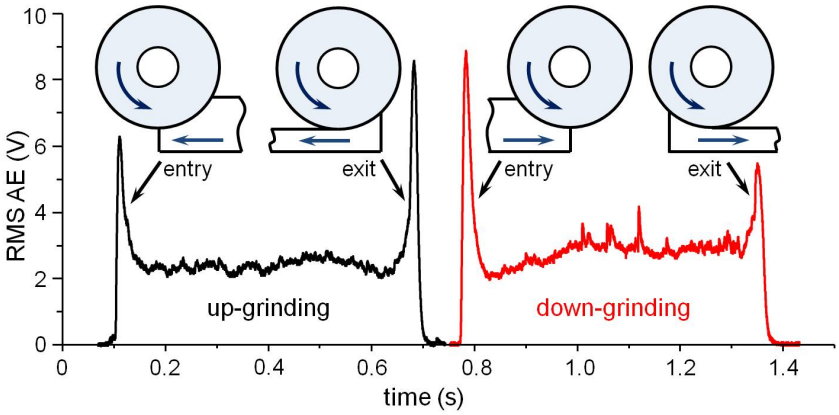

Fig. 2. Effect of grinding direction on entry and exit spikes.

Pursuing this lead, the effect of workpiece wedge angle Θ was examined (Fig. 3), in consideration of its profound influence on burr formation. Among the angles investigated, the spikes were the most prominent for $\Theta = 45°$, which corresponded to significant burr formation as well, as also noted in [8,9]. For the case of up-grinding, the entry and exit spikes appear to be of comparable magnitude for this wedge angle, as the AE signal was strong enough to have saturated the pre-amplifier; this is however of little consequence in this particular instance, as the intent was to investigate the relative spike heights with reference to workpiece geometry. The spike height can be seen to diminish dramatically as the wedge angle is increased to 135° and 175°, in both of which cases there were no burrs. In contrast, the 45° wedge angle workpiece rotated about its axis onto its side, so as to gradually engage and disengage the wheel across its width developed a sizeable burr, but with essentially no spikes.

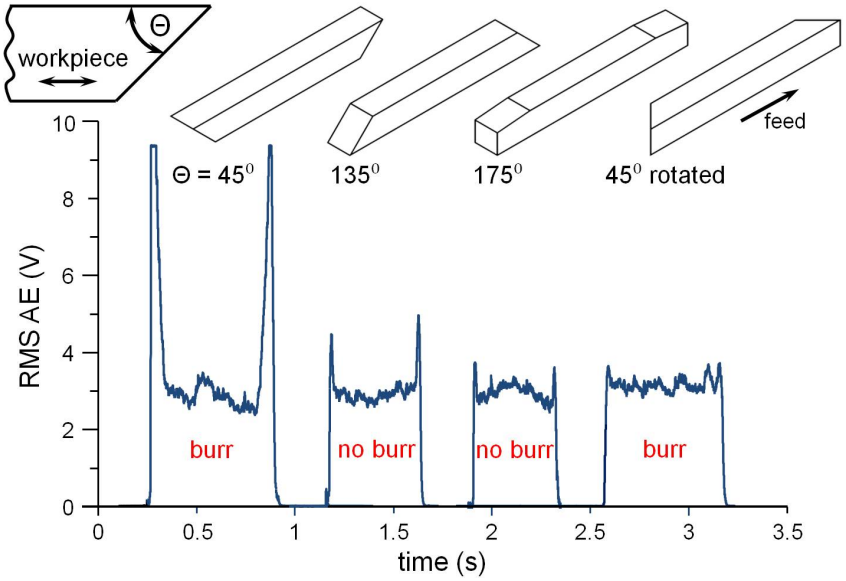

Fig. 3. Effect of workpiece edge geometry on spikes and burrs.

The existence of all the four possible combinations of the incidence of burrs and spikes (see Fig. 3) implies that their underlying mechanisms could operate independently. For a small workpiece wedge angle, as in when $\Theta = 45°$, burr formation is markedly enhanced due to the reduction in the rigidity of the edge, and the elevated temperature therein due to heat conduction being impeded by the relative lack of surrounding bulk material that would have acted as a heat sink [9]. In the case of the 45° workpiece rotated about its axis, the absence of spike formation hints at the potential effect of the dynamic response of the grinding system, considering that the engagement as well as the disengagement of the workpiece with the wheel is gradual, in comparison to the other three edge geometries. These aspects will be revisited in detail in the next subsection, which delves on the frequency content of the raw AE signal.

Referring to Figs. 2 and 3, the spikes can be seen to typically last several tens of ms, which is an order of magnitude longer than the times corresponding to the related burr lengths measured. This further confirmed that there was more to the spikes than just burr formation. Such extended durations moreover indicated the spikes to be basically unrelated to the burst signals from incipient engagement of the workpiece by the grits that protrude the most, as such features usually span just a few ms [6].

Observing the apparent decrease in the nominal spike duration with increasing wedge angle (Fig. 3), it transpired that the duration may be related to the wheel-work contact length. Tests were hence run to investigate this systematically by varying the depth of cut a_e on a workpiece with a 90° wedge angle. In order to objectively determine the spike duration in the RMS AE signal (say Fig. 4a), the corresponding instantaneous temporal slope was computed (Fig. 4b); the duration of the spike was obtained therefrom, as the time elapsed between the initiation of the spike and the second zero crossing in the slope characteristic, noting that the first zero crossing corresponds to the maximum spike amplitude.

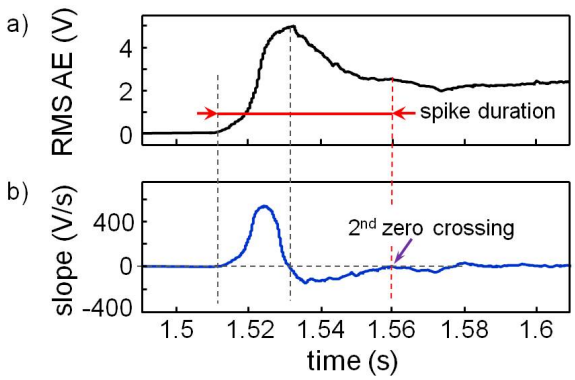

Fig. 4. Calculation of spike duration.

Fig. 5 presents the contact length estimated as the product of the spike duration and the table feed rate. Superposing these results on multiples of the geometric contact length l_g approximated as $\sqrt{a_e d_s}$ where d_s is the wheel diameter, it is evident that the estimated length, which is about $3l_g$ at the lower end of the depth of cut approaches $2l_g$ at the higher end. This is in exact conformance with the knowledge [10,11] that the actual nominal contact length in grinding is typically 2 to 3 times the geometric contact length due to elastic deformation in the contact zone [12], and that the ratio decreases with an increase in the depth of cut [13]. The values are as well in agreement with [11] that the difference in contact length between up- and down-grinding is on the same order as the inherent variability.

A comparison of the data in Fig. 5 with that of experimental values in Fig. 6 reported by Mao et al. [14] in the grinding of cast iron using a vitrified wheel for wheel and table speeds in the range of 20–30 m/s and 20–100 mm/s does indeed validate the application the RMS AE signal in estimating the actual contact length. Additional confirmatory tests showed an increase in contact length with table feed rate at a set depth of cut as is to be expected [10], on account of larger deformations associated with the higher grinding forces.

That the RMS AE signal presents a simple and novel method for estimating the actual contact length is of much practical significance, considering that its measurement by conventional techniques such as those that involve thermocouples are rather cumbersome and destructive. Knowledge of the actual contact length is invaluable in the prediction of grinding temperatures, as computations that refer to the geometric length instead return temperatures that are substantially in excess of the actual values.

It may be noted that the contact length estimated thus refers to the chordal distance parallel to the table feed direction, which is a reasonable approximation only at low depths of cut. Furthermore, the values would be higher if the workpiece wedge angle is less than 90° and vice versa. Spike durations are further influenced [15] by the integration time constant: for the value of 1.2 ms

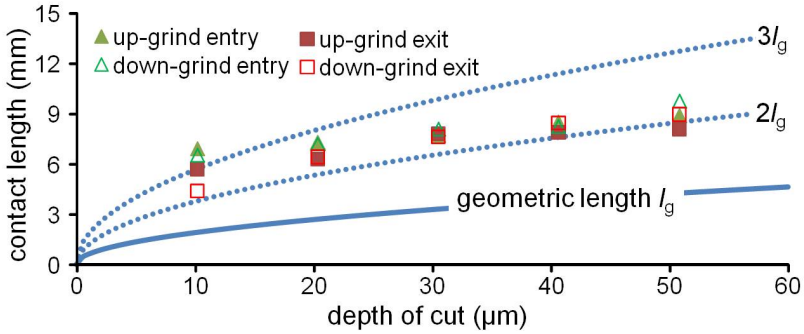

Fig. 5. Contact length estimated from spike duration.

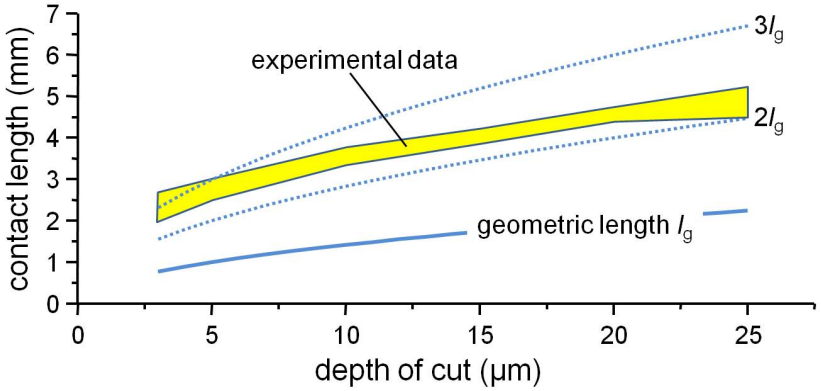

Fig. 6. Experimentally measured contact length (adapted from [14]).

used in this work, a sensitivity analysis showed the spike duration estimated from the RMS AE signal to be accurate to within less than 10% of the corresponding duration in the raw AE response. The AE signal is also preferably acquired directly on the workpiece, to minimise errors associated with possible reflections at any interfaces in the measurement chain, which tend to dilate the spikes in the RMS AE characteristic [15].

In order to understand the spikes appearing just at the entry/exit edges, the frequency content of the raw AE signal was investigated next to identify any differences in the spectral composition of the transient spikes relative to the continuous region sandwiched in between.

3.2 Analysis of raw AE signal

Figs. 7a, 7b and 7c show the frequency spectrum of the raw AE signal referring to the entry, continuous and exit regions, respectively. In all three regions, the signals comprise peaks clustered around about 85, 150 and 250 kHz, with little content beyond 400 kHz. Figs. 7d, 7e and 7f are the corresponding spectra with the only difference that the coolant flow was suspended to intentionally induce grinding burn. Examination of these spectra points to grinding burn having spurred an all around increase in AE activity, as has been reported in [2,6]. More specifically, closer inspection of Figs. 7b and 7e referring to the continuous region indicates grinding burn to have manifested prominent peaks in the vicinity of 150 kHz as exemplified in the corresponding figure insets, which signifies this band to refer to thermal damage.

To further confirm this hypothesis, an experiment was conducted to study the effect of juxtaposing a sacrificial workpiece to facilitate coolant ingress into the wheel-work interface during wet grinding, on this frequency range. To circumvent transient effects, AE was measured at a location 10 mm from the workpiece edge that is outside of the entry region, such that AE at this location is continuous. This experiment indicated a significant decrease in the

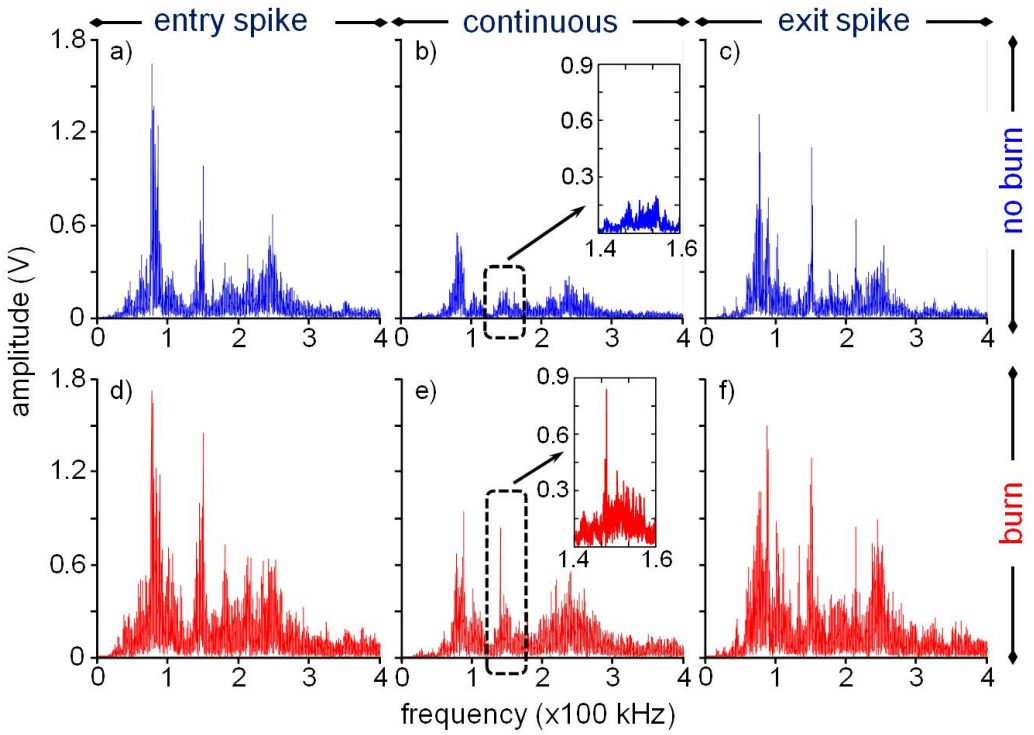

Fig. 7. Comparison of frequency content of the raw AE signal.

frequency content around 150 kHz on introduction of a sacrificial workpiece (Fig. 8b) compared to the one without (Fig. 8a), which conclusively indicated this band to refer to thermal effects.

That the 150 kHz band is prominent at the entry/exit edges (Figs. 7a and 7c, in contrast to Fig. 7b) even under conditions of no grinding burn suggests local thermal damage at the edges, conceivably due to the lack of sufficient

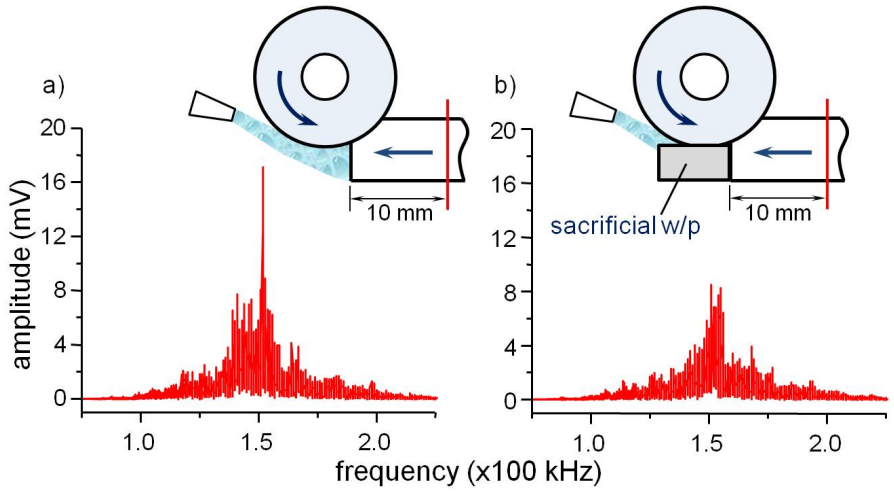

Fig. 8. Effect of a sacrificial workpiece on the AE frequency range referring to thermal effects.

material at the wedge to function as a heat sink. Such an effect has been found [16] to elevate the transient surface temperatures at the edges to above the steady-state values, which can be high enough to bring about localized thermal alteration of the material [9]. Thermal damage at the wedge is however not apparent on the generated surface as it is confined within the depth of material that is subsequently removed in the same grinding pass.

Fig. 9 shows the effect of edge angle on the contributions to the RMS AE signal from the 75–95 kHz and 140–160 kHz frequency bands. The amplitude of the spikes referring to thermal damage (140–160 kHz) can be seen to decrease as the edge angle is increased from 45° to 135°, evidently due to the additional material available at the workpiece wedge towards enhancing heat conduction.

AE around 100 kHz has been reported to refer to the dynamic response of the system in investigations relating to grinding [17] and broaching [5]. Along these lines, the amplitude of the spikes referring to the 75-95 kHz band, can also be seen in Fig. 9 to progressively decrease with an enhancement in the rigidity associated with the increase in the wedge angle from 45° to 135°, with it rendered largely non-existent for the 45° workpiece rotated about its axis so as to gradually engage the wheel. This validates the notion that the 75–95 kHz band refers to the dynamic system response, in terms of the transient mechanical loading and unloading associated with the engagement and disengagement of the work with the wheel.

In the signals shown in Fig. 9, the thermal and dynamic effects occur concurrently. In order to resolve and authenticate these effects, an experiment was designed to involve two workpiece geometric configurations. In the first case, a groove of width 1 mm and a depth of 0.5 mm was pre-machined into the workpiece (Fig. 10a), while the second case entailed two workpieces that were physically separated by the same width of 1 mm (Fig. 10b). As the gap of 1 mm is smaller than the actual contact length (>3 mm), the RMS AE

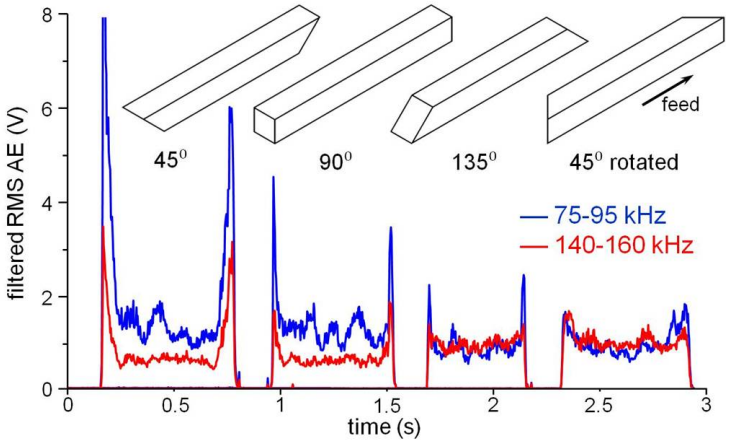

Fig. 9. Effect of workpiece wedge angle on filtered RMS AE.

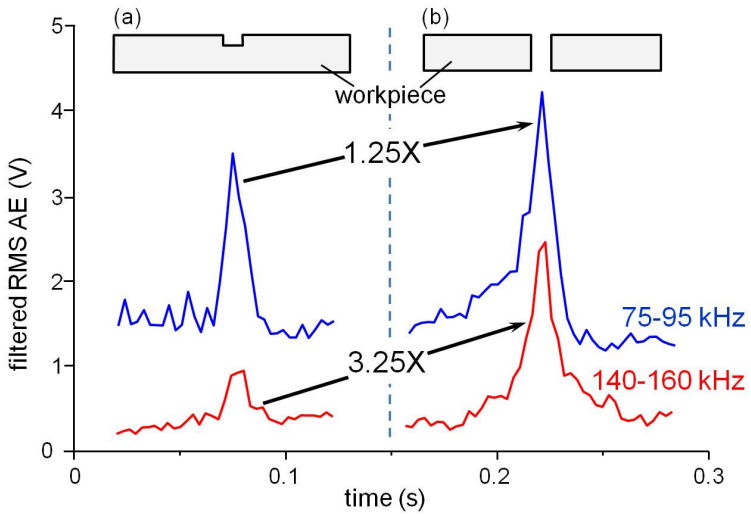

Fig. 10. Filtered RMS AE for different workpiece configurations.

signals exhibit a single peak that consolidates the contributions from the two edges. Given that the 1 mm gap is the same in both cases, the associated damping is largely the same as the wheel passes over and across the gap; the thermal damage, on the other hand, may be expected to be higher in the second case (Fig. 10b) as there is relatively less bulk material at the edges to absorb and conduct the heat. A comparison of the contributions from the dynamic (75–95 kHz) and thermal (140–160 kHz) components indicates this to be precisely the case (Fig. 10), as the latter entails an increase in the peak amplitude by a factor of 3.25, which is notably higher than the factor of 1.25 in the former.

Referring back to Fig. 9, the shape of the peaks in the signals referring to thermal damage (140–160 kHz) at entry is consistent with the enhanced heat transfer commensurate with the wheel progressively establishing contact with the workpiece over the actual contact length. The converse of this phenomenon occurs at the exit side as the wheel gradually loses contact with the workpiece and ultimately disengages. Such symmetric nature of the spikes between entry and exit indicates the settling characteristic of the AE sensor to have been of no influence. Similarly, the peaks in the signal referring to the system dynamics (75–95 kHz) at the entry and exit may be explicated in terms of the respective increase and decrease in the damping developed at the wheel-work interface, given that the level of damping is proportional to the wheel-work contact length [18]. This is essentially the same mechanism behind the decrease in the amplitude of the RMS AE signal with the progression of tool flank wear in cutting [2].

The discussions thus far have focussed on the 75–95 kHz and 140–160 kHz frequency bands. A comparison of the RMS AE characteristics of the third dominant frequency band in the range of 240–260 kHz (see Fig. 7) with that

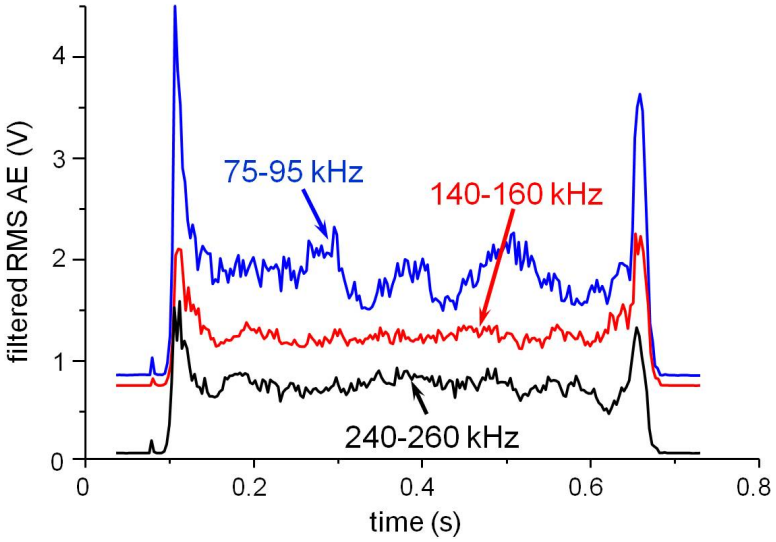

Fig. 11. Comparison of dominant frequency bands.

of the other two (shown vertically displaced for clarity in Fig. 11), shows the 140 – 160 kHz and 240–260 kHz bands to comprise features that closely resemble each other, while the 75–95 kHz band is noticeably dissimilar. This denotes the former two bands to be of thermal origin, which concurs with [17,19–21] that thermal effects in grinding generate AE at frequencies higher than 100 kHz.

4 Conclusions

The spikes in the AE signal that correspond to the workpiece entry and exit have been investigated with regard to both the RMS and raw AE signals, in the surface grinding of hardened high speed steel. Burr formation was found to be only weakly correlated to the spike occurrence. For a workpiece with a wedge angle of 90°, the length associated with the duration over which the spikes are sustained has been shown to correspond to the actual wheel-work contact length in grinding. This presents the prospect for a simple and non-destructive test method, which is of great significance, for instance, in the estimation of grinding temperatures. Additional experimental work is warranted to validate the proposed technique against conventional ones.

An investigation of the effect of the workpiece wedge angle has indicated the transient spikes at the entry and exit to be a consequence of the wheel establishing and losing contact with the work over the actual contact length, in terms of heat conduction and damping, which are shown to be reflected in characteristic frequency bands of the AE signal. This underlines the significant potential for further expanding the scope of AE as a tool for detecting grinding damage in a wide range of workpiece materials, and for characterizing the dynamic response of a grinding system.

Acknowledgements

This research was funded by the Natural Sciences and Engineering Research Council of Canada. P. Koshy acknowledges a Fellowship from the Alexander von Humboldt Foundation.

References

[1] D.E. Lee et al., Precision manufacturing process monitoring with acoustic emission, *International Journal of Machine Tools and Manufacture* 46 (2006) 176–188.

[2] H.K. Tönshoff, I. Inasaki, *Sensors in Manufacturing*, Wiley-VCH Verlag, Weinheim (2001).

[3] B. Karpuschewski, M. Wehmeier, I. Inasaki, Grinding monitoring system based on power and acoustic emission sensors, *CIRP Annals* 49 (2000) 235–240.

[4] E.N. Dei, D.A. Dornfeld, Acoustic emission from face milling process—the effects of process variables, *Journal of Engineering for Industry*, 109 (1987) 92-99.

[5] D.A. Axinte, N. Gindy, K. Fox, I. Unanue, Process monitoring to assist the workpiece surface quality in machining, *International Journal of Machine Tools and Manufacture* 44 (2004) 1091–1108.

[6] J. Webster, I. Marinescu, R. Bennett, Acoustic emission for process control and monitoring of surface integrity during grinding, *CIRP Annals* 43 (1994) 299–304.

[7] J.F.G. Oliveira, C.M.O. Valente, Fast grinding process control with AE modulated power signals, *CIRP Annals* 53 (2004) 267–270.

[8] S. Kawamura, J. Yamakawa, Formation and growing up processes of grinding burrs, *Bulletin of the Japan Society for Precision Engineering*, 23 (1989) 194–199.

[9] J.C. Aurich, H. Sudermann, H. Bil, Characterisation of burr formation in grinding and prospects for modelling, *CIRP Annals* 54 (2005) 313–316.

[10] J. Verkerk, The real contact length in cylindrical plunge grinding, *CIRP Annals* 24 (1975) 259–264.

[11] J. Wager, D. Gu, Influence of up-grinding and down-grinding on the contact zone, *CIRP Annals* 40 (1991) 323–326.

[12] W.B. Rowe et al., The effect of deformation on the contact area in grinding, *CIRP Annals* 42 (1993) 409–412.

[13] W.B. Rowe, *Principles of Modern Grinding Technology*, William Andrew Publishers, Oxford (2009).

[14] C. Mao, Z. Zhou, D. Zhou, D. Gu, Analysis of the influence factors for the contact length between wheel and workpiece in surface grinding, *Key Engineering Materials* 359–360 (2008) 128–132.

[15] K. Jemielniak, Some aspects of acoustic emission signal pre-processing, *Journal of Materials Processing Technology* 109 (2001) 242–247.

[16] C. Guo, *Investigation of Fluid Flow and Heat Transfer in Grinding*, Doctoral Thesis, University of Massachusetts, Amherst (1993).

[17] J. Griffin, X. Chen, Multiple classification of the acoustic emission signals extracted during burn and chatter anomalies using genetic programming, *International Journal of Advanced Manufacturing Technology* 45 (2009) 1152–1168.

[18] I. Inasaki, B. Karpuschewski, H. Lee, Grinding chatter—Origin and suppression, *CIRP Annals* 50 (2001) 515–534.

[19] H. Eda et al., In-process detection of grinding burn by means of utilizing acoustic emission, *Bulletin of the Japan Society for Precision Engineering* 18 (1984) 299–304.

[20] W. König, T. Klumpen, Monitoring and sensor concepts for higher process reliability, *SME Technical Paper* MR93-358 (1993) 1–23.

[21] Q. Liu, X. Chen, N. Gindy, Investigation of acoustic emission signals under a simulative environment of grinding burn, *International Journal of Machine Tools and Manufacture* 46 (2006) 284–292.